The Growth Mechanism, Thermal Stability, and Reactivity of Palladium Mono- and Multilayers on Cu(110)

J. P. Reilly and C. J. Barnes

School of Chemical Sciences, Dublin City University, Glasnevin, Dublin 9, Ireland

N. J. Price, R. A. Bennett, S. Poulston, P. Stone, and M. Bowker*

Department of Chemistry, University of Reading, Whiteknights Park, Reading, RG6 6AD, United Kingdom

Received: January 12, 1999; In Final Form: May 20, 1999

The room-temperature growth of palladium (Pd) on Cu(110) has been studied by X-ray photoelectron spectroscopy (XPS), scanning tunneling microscopy (STM), low-energy electron diffraction (LEED), and temperature-programmed desorption (TPD). XPS signal versus deposition time plots rule out a simple layer-by-layer growth mechanism. STM/LEED indicates formation of regions of (2 × 1) overlayer at low Pd coverages ($\theta_{Pd} < 1$ ML), with considerable disorder in the form of monolayer deep pits and islands. Higher Pd coverages lead to the formation of a granular film consisting of densely packed, flat-topped Pd clusters of average size 75 × 150 Å and with largely a rectangular shape. The favored growth mechanism is of multilayered Pd islands above a mixed (2 × 1) CuPd interface of two to three atomic layers thickness. The thermal stability of the Pd/Cu(110) system was investigated with XPS peak intensity versus annealing temperature plots that indicate that bulk intermixing takes place rapidly between 500 and 600 K. The Pd $3d_{5/2}$ XPS peak widths narrow, suggesting the formation of a largely homogeneous CuPd surface alloy. STM indicates that heating to 500 K leaves the Pd clusters in a largely unaltered morphology with no sign of Ostwald ripening, whereas annealing to 600 K leads to considerable changes in topography. The granular structure of the Pd film is disrupted, leading to a surface with irregularly shaped flat domains separated by mono-atomic steps. High temperature (720 K) annealing leads to further flattening and appearance of regular parallel lines in STM images. The spacing of these lines varies with Pd loading, and they are assigned to strain due to lattice mismatch between the "capping" copper monolayer and the underlying mixed CuPd alloy. The reactivity of the Pd/Cu(110) surface has been probed by dosing formic acid and monitoring formate decomposition. High Pd coverages lead to a substantial destabilization of the formate relative to clean Cu(110), which is assigned to formate adsorption on mixed CuPd sites.

1. Introduction.

Surface alloys are a class of structure that can be formed by evaporation of one metal onto a second material with substitution of the adsorbate into the outermost few atomic layers of the substrate yielding a mixed and often ordered array. Study of surface alloys is motivated by the understanding of the influence of a thin intermixed alloy "buffer" layer in subsequent epitaxial growth and the use of surface alloys as model substrates to study the effect of alloying on gas adsorption and surface-catalyzed reactions.[1,2]

To date most effort has been devoted to characterization of the structure and chemical reactivity of submonolayer metal coverages, forming either an outermost single layer or bilayer mixed surface. There are many examples where adsorbate reactivity on alloys falls between that of the two metals.[1] However, less is known about subsequent growth at higher metal loading, how the mixed bimetallic interface influences the subsequent growth mode of the film, and how the resulting film affects catalytic activity.

Of all the bimetallic combinations, CuPd has received considerable attention because of its use industrially for CO and alkene oxidation,[3] ethanol decomposition,[4] and CO, benzene, and toluene hydrogenation.[5] Copper (Cu) and palladium (Pd) form binary alloys throughout the composition range, including both ordered and substitutionally disordered alloys.[6,7] Upon alloying, valence level photoemission reveals profound effects on the local electronic structure of Pd in dilute CuPd alloys in the form of withdrawal of the high density of d-states at the Fermi level, which is characteristic of pure Pd and due to d-to-sp rehybridization and charge transfer. This withdrawal of d-states has the effect of making Pd behave like a closed d-band metal in its surface chemical behavior.[8,9] Recent studies have also indicated interesting lattice distortions in the selvedge of CuPd alloys.[10]

In general, ordered surface alloy formation occurs more readily in the case of growth of high melting point/surface energy metals (e.g., Pd) onto lower surface energy substrates (e.g., Cu). A considerable amount of work has been done on the opposite combination (i.e., Cu deposition on Pd single-crystal surfaces[11−14]) where two-dimensional monolayer formation is favored. For deposition at 300 K, strained epitaxial overlayers are formed with little intermixing, alloying occurs only at elevated temperatures, and ordered surface alloy formation between Cu and Pd is generally not observed. In contrast, Pd deposition onto Cu single-crystal surfaces leads to ordered

* Corresponding author. E-mail: m.bowker@reading.ac.uk. FAX: +44-(0)118 9316 331.

10.1021/jp990156p CCC: $18.00
Published on Web 07/20/1999

surface alloys via place exchange of the Cu substrate with Pd atoms in the outermost layers, this order is favored both by the enhanced kinetics due to the relative ease of breaking Cu−Cu bonds compared with Pd−Pd bonds and the additional thermal energy of the incoming hot Pd atoms. The Cu(100) substrate has received the most attention[15] and reveals formation of a c(2 × 2) CuPd surface alloy upon deposition of submonolayer Pd coverages at 300 K via substitution of Pd adatoms into the outermost layer. However, the surface formed is heterogeneous, with domains of top layer c(2 × 2) alloy and patches of (1 × 1) pure Cu at coverages at which the c(2 × 2) reaches its maximum perfection in low-energy electron diffraction (LEED).[16,17] Less work has been performed on the Cu(110) surface. Aside from an early LEED study by Fujinaga,[18,19] the only detailed study to date is that of Murray et al.[20] who utilized scanning tunneling microscopy (STM) to study the growth mechanism and structure of Pd films at low coverage (up to 0.3 ML). Low Pd coverage leads to substitution of Pd atoms into the outermost Cu layer forming an ordered (2 × 1) CuPd surface alloy via periodic substitution of every second Cu atom along the [1$\bar{1}$0] rows by Pd, with expelled Cu atoms diffusing to step edges. As the Pd coverage increases, larger domains of (2 × 1) alloy form and are covered by a monolayer of Cu originating both from step edges and from the Cu(110) terraces that exhibit monolayer deep "pits". It appears that a subsurface, second layer (2 × 1) CuPd alloy covered by a copper monolayer is the stable structure at higher Pd coverages. The CuPd (2 × 1) chains formed at low Pd coverage ($\theta_{Pd} = 0.17$ ML) remain uncovered because of the necessary formation of a large number of high-energy Cu edge atoms in a small two-dimensional (2D) island that would be required to "cap" the chain. Although Murray et al.[20] studied Pd coverages up to only ≈0.3 ML, it appears reasonable that at coverages of 0.5 ML, large areas of a copper-capped p(2 × 1) CuPd underlayer will be the dominant structure, with the top two layers having a similar structure to that determined for a bulk $Cu_{0.85}Pd_{0.15}$(110) alloy.[21]

Little is known about the growth mechanism and structure of Pd on Cu(110) at coverages above 0.3 ML. In a short communication[10] we have outlined a number of aspects of the growth of Pd on Cu(110) for coverages above 0.5 ML, indicating a growth model in which further alloying occurs, with the outermost copper monolayer forming a bi- or trilayer of CuPd alloy upon which pure Pd eventually grows in the form of flat-topped epitaxial platelets. The aim of this study is to extend the work of Murray et al. by looking at the room-temperature growth for higher Pd coverages, probing the thermal stability of the Pd/Cu(110) layers by STM and X-ray photoelectron spectroscopy (XPS), and examining the surface reactivity of the composite CuPd layers by monitoring the thermal stability of a reactive intermediate (i.e., a formate species formed by adsorption of formic acid).[22]

2. Experimental Section

Experiments were performed in two separate ultrahigh vacuum (UHV) chambers operated at base pressures in the low 10^{-10} Torr range. The first chamber was equipped with LEED optics for surface crystallographic characterization and unmonochromated XPS (single-channeltron angle-resolved analyzer) facilities coupled with a Vacuum Generators quadrupole mass spectrometer (MS) for both monitoring gas purity and detecting temperature-programmed desorption (TPD). The second chamber consisted of a variable temperature Oxford Instruments STM. This STM system was also equipped with a quadrupole MS and was accompanied by LEED characterization facilities that also served as a retarding field analyzer for surface elemental characterization by Auger electron spectroscopy (AES).

The Cu sample was oriented to within 0.5° of the (110) plane (Metal Crystals and Oxides Ltd.). Cleaning of the sample typically involved repeated cycles of argon-ion bombardment, initially with the sample at room temperature and finally at ∼700 K. Upon ceasing ion bombardment, the sample was annealed in UHV at ∼700 K for several minutes to restore surface order, which produced a sample surface that exhibited a sharp low background (1 × 1) LEED pattern. XPS and AES indicated no contaminants above their respective noise limits.

A standard TPD setup comprised of line-of-sight geometry between sample and MS as well as a linear sample heating rate (∼1.5 K s^{-1}), was employed. Formic acid (97% purity, Aldrich Chemicals Ltd.) dosing was carried out via a liquid reservoir attached to a fine control leak valve and was checked for purity with the quadrupole MS. Gas exposures were measured with an uncalibrated Bayard-Alpert ionization gauge and are quoted in Langmuirs (1 Langmuir = 10^{-6} Torr s). All XPS experiments were recorded using Al−Kα radiation ($h\nu = 1486.6$ eV) with XPS binding energies referenced to the Cu $2p_{3/2}$ core-level intensity at 932.7 eV.[23] The electrostatic hemispherical analyzer was operated with a fixed analyzer transmission energy of 44 eV (FAT mode). The accuracy of the measured binding energies is ± 0.1 eV.

Palladium was evaporated using a home-built sublimation source. This evaporation was achieved via the resistive heating of a 0.3 mm diameter tungsten filament around which a 0.125 mm diameter high purity Pd wire (Goodfellows Metals Ltd.) was wound. The evaporators were outgassed until they could be used with the chamber pressure remaining in the 10^{-10} Torr range. Deposited films were shown, by XPS/AES analysis, to be spectroscopically pure with homogeneous Pd coverage across the entire surface. Palladium deposition rates (∼2 × 10^{-3} ML s^{-1}) were calibrated as follows: for all TPD experiments the deposition rate was monitored by recording the ratio of the Pd $3d_{5/2}$ [kinetic energy (KE) ∼1150 eV] and Cu $2p_{3/2}$ (KE ∼550 eV) core-level intensities as a function of evaporation time. In the STM chamber, the growth rate of Pd on Cu(110) was estimated by construction of Auger signal versus evaporation time (AS−t) plots. These plots were afforded by monitoring the ratio of the peak-to-peak amplitudes of the derivative spectra of the Pd $M_{4,5}N_{4,5}N_{4,5}$ (KE = 326, 330 eV) and the Cu $M_{2,3}VV$ (KE = 59, 61 eV) Auger transitions employing the LEED optics as a retarding field analyzer (RFA). We estimate the coverages quoted should be accurate to within about ±50% between chambers.

3. Results and Discussion

3.1. Room-Temperature Growth Mechanism − Pd/Cu-(110). Figure 1 shows a plot of Pd $3d_{5/2}$/Cu $2p_{3/2}$ XPS intensities ratio for incremental Pd doses on Cu(110). The areas plotted are integrated peak areas after a linear background subtraction. The data were recorded at a takeoff angle of 40°. Use of a ratio rather than plotting Cu or Pd peak intensities individually serves to remove errors in repositioning the sample after evaporation and changes in X-ray flux. All evaporations were carried out with the sample held at room temperature (300 K). On the same graph we show the theoretical layer-by-layer (Frank van der Merwe) growth curve for Pd on Cu(110). The theoretical ratios

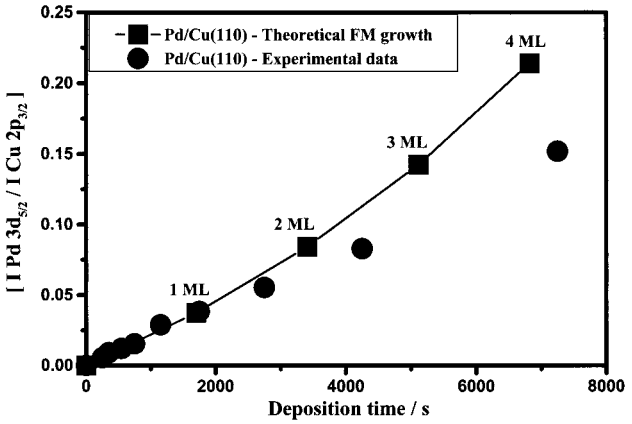

Figure 1. Ratio of the variation of the integrated area of the Pd $3d_{5/2}$ core level to that of the Cu $2p_{3/2}$ level (open circles) for deposition of Pd onto Cu(110) at 300 K. Also shown is a theoretical prediction for a perfect layer-by-layer (Frank van der Merwe = FM) growth mechanism.

are calculated from eq 1:

$$\frac{I_{\mathrm{Pd}}}{I_{\mathrm{Cu}}} = \frac{I^{\infty}_{\mathrm{Pd}}}{I^{\mathrm{o}}_{\mathrm{Cu}}}\left[\frac{1 - \exp\left[\frac{-d}{\lambda_{\mathrm{Pd}}\cos\theta}\right]}{\exp\left[\frac{-\mathrm{d}}{\lambda_{\mathrm{Cu}}\cos\theta}\right]}\right] \qquad (1)$$

Where I^{∞}_{Pd} is the Pd $3d_{5/2}$ signal from a "bulk" Pd overlayer, I^{o}_{Cu} is the Cu $2p_{3/2}$ intensity from the clean Cu(110) crystal, θ is the emission angle of the electrons with respect to the surface normal ($\theta = 40°$), and d is the distance travelled through the Pd overlayer by the emitted electrons (Å). A "bulk" Pd overlayer was considered to be an overlayer of sufficient thickness to completely damp the XPS signal from the underlying copper substrate. The terms λ_{Pd} and λ_{Cu} are the inelastic mean free paths (IMFP) of the Pd $3d_{5/2}$ and the Cu $2p_{3/2}$ core-levels, which were calculated to be 16.7 and 10.5 Å, respectively, using the formalism of Seah and Dench.[24]

It is known that for coverages at least up to 0.3 ML, Pd essentially grows two-dimensionally via substitution into the top copper layer of the substrate forming a (2 × 1) CuPd surface alloy.[20] Therefore, the theoretical layer-by-layer growth curve was fitted to the experimental curve at low Pd coverage. It is anticipated that a small error will exist in quoted coverages using a fitting of this type because the majority of Pd atoms, although growing in a 2D layer, are covered by a copper monolayer as outlined in the *Introduction*. This error will serve to make the actual coverages of Pd on the surface slightly higher than that predicted by Figure 1. A simple calculation based on comparing a 0.5 ML Pd film in a true layer-by-layer growth mode and in a copper-coated subsurface (2 × 1) layer indicates that coverages would be underestimated by ≈15%. All coverages quoted have thus been adjusted for this effect. It should be stressed that even after this adjustment, the XPS coverages quoted must only be viewed as estimates because of uncertainties in the inelastic mean free paths utilized and possible photoelectron diffraction effects within the film leading to enhancements or reductions of the measured XPS signal from geometric rather than compositional effects. It would seem reasonable to assume that the quoted absolute coverages are accurate to within ±50%.

Inspection of Figure 1 illustrates that the experimental data fall below that predicted for pure layer-by-layer growth. This result clearly signals departure from simple 2D growth already at coverages around 1 ML. This departure is not surprising because the Pd surface energy (2.043 J m^{-2}) is higher than that of Cu (1.934 J m^{-2}),[25] which, along with the 7.7% lattice mismatch, favors a growth mechanism in the form of clusters. The higher surface energy of Pd is verified experimentally by the work of Murray and co-workers who found that the (2 × 1) CuPd alloy prefers to be covered by a copper monolayer,[20] growth of Cu on Pd(110) is 2D up to completion of the first atomic layer,[11] and the bulk alloy is Cu terminated.[21]

The XPS data shown in Figure 1 indicate that the Pd:Cu XPS ratio increases in a near linear fashion. This linearity may be explained if at coverages beyond 1 ML a linear increase in the Pd cluster density occurred as a function of evaporation time with little change in the cluster base-to-height ratio. The clusters must have a high base-to-height ratio, hence mimicking quite closely layer growth. Due to the propensity for the Pd/Cu(110) system to mix for 300 K deposition, it is likely that at coverages > 0.5 ML, further intermixing with the outermost copper monolayer, will occur initially, as postulated by Murray et al. at lower coverages.[20] This intermixing will lead to growth of a second mixed CuPd layer above the (2 × 1) CuPd surface alloy. This mixing will clearly be limited, as the amount of copper directly available for further alloying is the single outermost monolayer capping the (2 × 1) CuPd alloy. It would appear likely that two or three alloyed layers may form prior to nucleation of pure Pd clusters signaled by the deviation from the theoretical curve between 1 and 2 ML coverage.

The adsorption of Pd was also followed qualitatively by observing changes in the LEED pattern with increasing Pd exposure at 300 K in the STM chamber. The Cu(110) surface exhibited a sharp low background (1 × 1) LEED pattern. Exposure to Pd led initially to an increase in diffuse background intensity before the formation of a p(2 × 1) LEED pattern as expected from the surface alloy.[18,26] The quality of the p(2 × 1) increased, although for deposition at 300 K there always remained clear signs of disorder evidenced by high background and the rather weak nature of the superlattice beams. Streaking and elongation of the (2 × 1) beams in the [001] direction was observed, suggesting poor long-range order of the (2 × 1) CuPd alloy in this direction. Increasing the Pd coverage beyond 1 ML led to a further increase in diffuse background scattering and a gradual weakening of the half-order beams. At high coverages, only a poor quality (1 × 1) pattern is observed. Figure 2 illustrates schematically the postulated growth mode involving nucleation of Pd clusters above a mixed (2 × 1) CuPd alloy "buffer" layer.

Figure 3 illustrates the evolution of the Pd 3d core level with increasing Pd coverage. A small shift to lower binding energy of 0.3 ± 0.1 eV and broadening is also observed with increasing coverage. The observed changes in XPS line shape are in agreement with the postulated growth mechanism. At lower coverages (up to ~1 ML), emission is predominantly from Pd in a CuPd alloy environment (higher binding energy XPS peak), whereas for higher coverages, emission occurs from both Pd in the mixed alloy buffer layer and metallic Pd clusters above the mixed interface. The observed broadening may thus be assigned both to the convolution of the chemically shifted "alloyed" Pd and metallic Pd but also to the larger width of the Pd core level in an epitaxial film than in an alloyed state (see *Thermal Stability* section). We postulate that the range of differing local geometries in the epitaxial film leads to a wider range of core binding energies than in a CuPd alloy for which all Pd atoms are in a similar local environment.

The observation of a shift to lower binding energy as the Pd coverage is increased agrees with the previous observations of

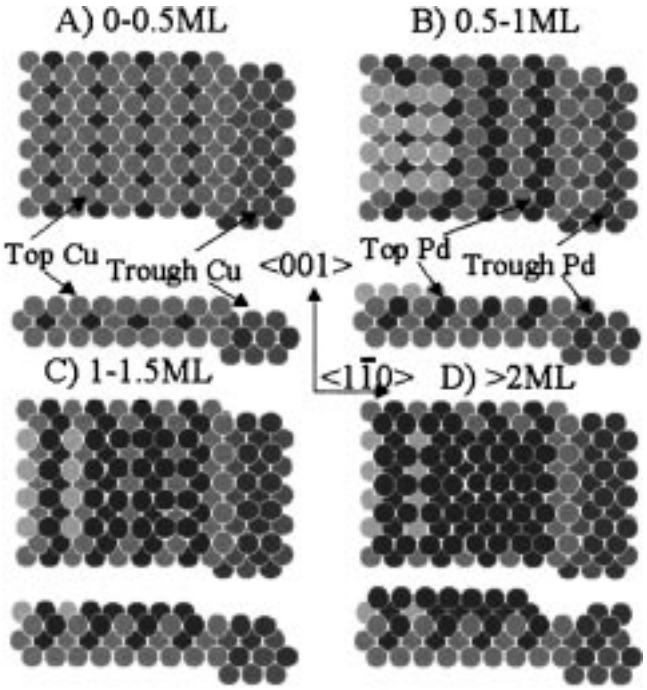

Figure 2. Schematic model of the suggested growth mechanism of Pd on Cu(110) at 300 K.

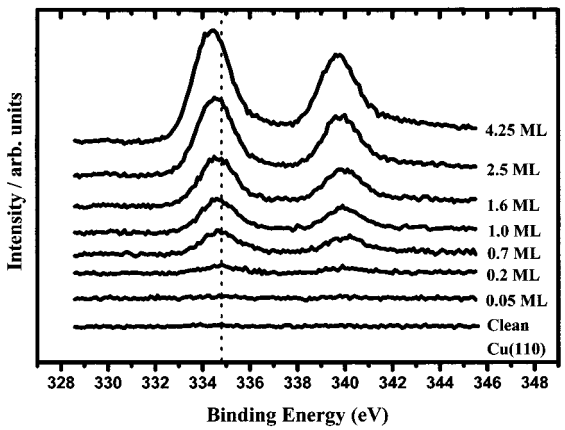

Figure 3. Palladium 3d core-level spectra as a function of surface coverage for Pd films grown on Cu(110) at 300 K. The dotted line is to aid visualization of the core-level chemical shift with increasing coverage.

Pope et al.[26] They report that a c(2 × 2) CuPd alloy formed on Cu(100) at Pd coverages of 0.5 ML have a 0.4 eV higher binding energy than for 2 and 4 ML Pd films. Pope's value agrees with the measurements of Graham et al.[27] who reported a +0.3 eV shift. Pope et al. also noted an increase in the full-width-at-half-maximum (fwhm) as the Pd coverage is increased that they attribute to a similar reason as our own assignment (i.e., a range of different environments for Pd).

To examine the room-temperature growth mechanism at a nanoscopic level, STM was applied. The STM images were recorded in constant-current mode for a range of Pd coverages with each film being freshly prepared by deposition at 300 K. Figure 4 illustrates a selection of STM images for increasing Pd coverage from submonolayer to thick films. Crystal orientation as indicated in Figure 4 is the same for all subsequent images shown.

Figure 4a reveals a 100 × 100 nm image of a 1 ML Pd film. The surface is highly heterogeneous and consists of monolayer deep pits, terraces, and monolayer high islands. The edges of the islands and terraces are not aligned in any ordered way. Figure 4b illustrates a 10 × 10 nm image at atomic resolution, indicating widespread formation of a (2 × 1) structure both within the islands and on terraces. These images suggest that for Pd coverages >0.5 ML, further alloying occurs and leads to formation of large areas of surface with a mixed CuPd (2 × 1) alloy layer outermost. This result is in direct contrast to the findings of Murray et al., who for lower coverages find that the (2 × 1) mixed layer is capped by a Cu monolayer. We suggest that for coverages beyond 0.5 ML (where the surface is dominated by the aforementioned CuPd underlayer capped by a Cu monolayer) arriving Pd atoms substitute within the outer Cu monolayer, thus forming a top layer (2 × 1) alloy. Ejected Cu atoms form islands above the alloyed double layer which may themselves mix with further Pd atoms arriving at higher coverages. Unlike the case at submonolayer Pd coverages, no surface Cu is available for alloying once the "capping" Cu monolayer has been used up. Figure 4c illustrates a 200 × 200 nm image of a 2.5 ML Pd film showing a surface upon which Pd clusters have begun to nucleate above the CuPd alloyed buffer layer. The image shows a high density of platelets covering a large fraction of the surface with monolayer and in some cases bilayer heights. The platelets adopt a range of shapes and sizes and there is clearly significant heterogeneity within the surface as would be expected; the 1 ML film does not present an ideal template upon which further Pd clusters may grow. Figure 4d illustrates a 100 × 100 nm image of a 4 ML Pd film, which clearly indicates growth of densely packed multilayered Pd platelets. The clusters are predominantly rectangular in shape and aligned with their edges parallel to the two high symmetry directions within the Cu(110) substrate. The clusters are now multilayered with a high base-to-height ratio that readily explains that although the XPS$-t$ plots do differ from that expected for a simple layer-by-layer growth mode, the deviation is not strong. Finally, Figure 4e (100 × 100 nm) illustrates an image from a "thick" (~10 ML) Pd film indicating a high density of densely packed clusters, separated by crevices. The clusters are predominantly flat topped in shape, and the film has a clearly granular appearance.

3.2 Thermal Stability of the Pd/Cu(110) System. To investigate the thermal stability of the bimetallic interface, the ratio of the Pd $3d_{5/2}$ to Cu $2p_{3/2}$ XPS core lines were monitored as a function of annealing for 30 s to increasingly high temperature (with XPS spectra being recorded on cooling to 300 K). Figure 5 reveals the resulting data for 3 and 8 ML films. In the case of the thinner film, the XPS ratio remains relatively constant up to ~500 K, after which a sharp drop is observed clearly illustrating that bulk alloying is rapid on an experimental time scale for temperatures >500 K. In the case of the 8 ML film, signs of intermixing occur even earlier at ~450 K.

Figure 6a illustrates the effect of annealing on the Pd 3d XPS core lines, again for a 3 and 8 ML film. In both cases the unannealed film exhibits a binding energy of 334.4 ± 0.05 eV. The binding energies and fwhm remain constant for annealing up to 473 K, after which a shift toward higher binding energy occurs along with a concomitant decrease in peak intensity due to thermally induced intermixing. Heating to 725 K leads to an intermixed alloy surface with a large shift of 0.6 ± 0.1 eV to higher binding energy relative to the as-deposited film and a marked reduction in fwhm. The XPS core level shift appears to mirror that reported for the Pd valence levels upon alloying with Cu during which a shift in the centroid of the d-band emission to higher binding energy occurs. The 4d valence level peaks at ~0.6 eV below the Fermi level in pure Pd, whereas in

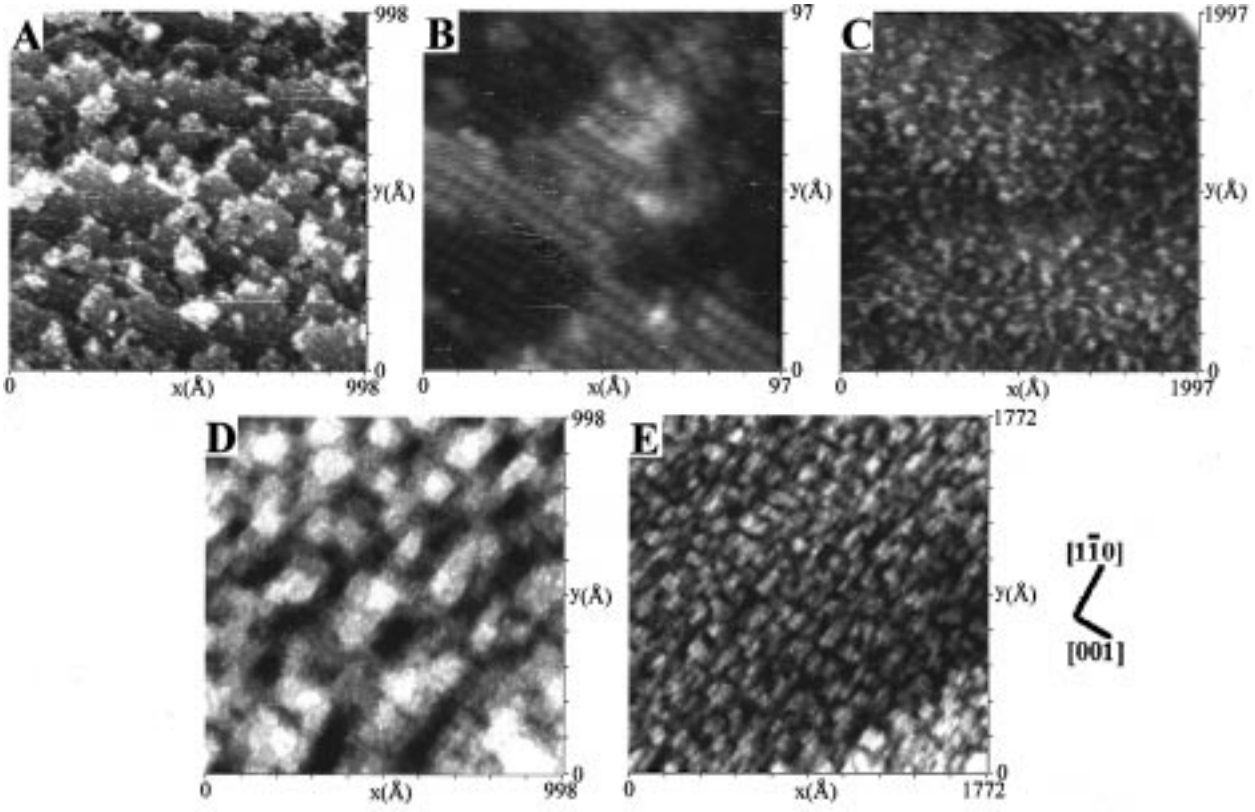

Figure 4. A series of representative STM images for Pd adsorption on Cu(110) at 300 K: (a) and (b) 1 ML; (c) 2.5 ML; (d) 4 ML; and (e) 10 ML. Tunneling current = 1 nA (all images), bias voltage = −500 mV (a,b) and 500 mV (c−e).

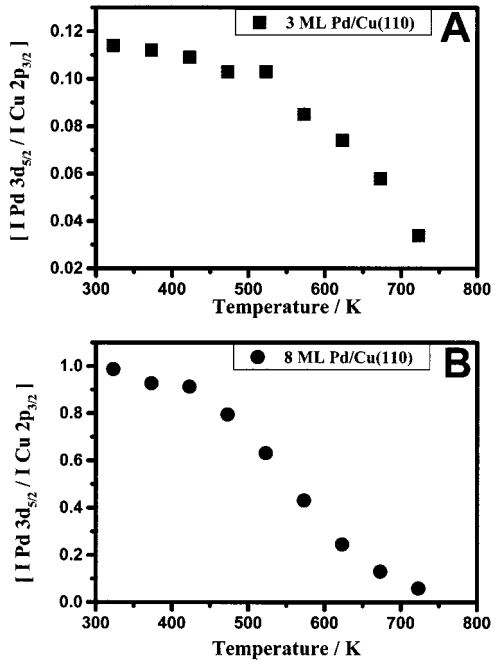

Figure 5. Variation of the background subtracted XPS Pd $3d_{5/2}$-to-Cu $2p_{3/2}$ core level ratio as a function of annealing temperature for (a) 3 and (b) 8 ML Pd films. In each case, the sample was held at the annealing temperature for 30 s and re-cooled to room temperature prior to the measurement.

a CuPd surface alloy of Cu:Pd local stoichiometry varying between 3:1 to 20:1, it is located at ∼1 eV higher binding energy.[28] Shifts in the valence and core levels in the same direction (but not necessarily of exactly the same magnitude) have been observed for a range of metal-on-metal systems.[29,30]

Figure 6b clearly illustrates the change in fwhm, which is a decrease of 0.2 eV that occurs predominantly between 500 and 600 K. The decrease in fwhm is somewhat sharper than the loss in intensity of the Pd XPS peak (Figure 5) and may suggest that although alloying is essentially complete by 600 K (leading to a reduction in fwhm), the continued drop of the XPS ratio in Figure 5 simply reflects slow diffusion of alloyed Pd deep into the crystal and out of the region probed by XPS (∼30 Å, ∼3λ). The reduction in fwhm is interpreted as being due to emission from Pd in a single alloy environment for high-temperature annealed films as opposed to the range of environments within the multilayer film with a corresponding range of core-level binding energies (cluster surface atoms, cluster bulk atoms, substrate cluster interface atoms, and intermixed buffer layer Pd).

Finally, Figure 7a illustrates the effect of annealing an 8 ML Pd film on the substrate Cu $2p_{3/2}$ core level and its fwhm. As expected, the Cu intensity begins to increase for annealing temperatures >475 K as diffusion is activated with a clear increase in peak position by 0.3 ± 0.1 eV attributable to CuPd alloying. Figure 7b illustrates a clear decrease in fwhm of 0.2 to 0.4 eV upon alloying, with the final value equal to that of clean Cu(110).

These shifts in peak maximum and fwhm agree with the measurements of Pope et al.[26] They report a decrease in binding energy of the Cu $2p_{3/2}$ core level of 0.25 eV relative to clean Cu(100) for deposition at 300 K, with an accompanying increase in fwhm. Pope et al. postulate that this result is due to surface alloying between Cu and Pd. Thus, the observed increase in binding energy in this case is interpreted as production of clean copper or alloy very dilute in Pd by heating to high temperature. The decrease in fwhm may in a similar way be interpreted as emission from a single pure Cu-like environment after high temperature annealing as opposed to a range of mixed (pure Cu, CuPd alloy etc.) environments in the as-deposited films.

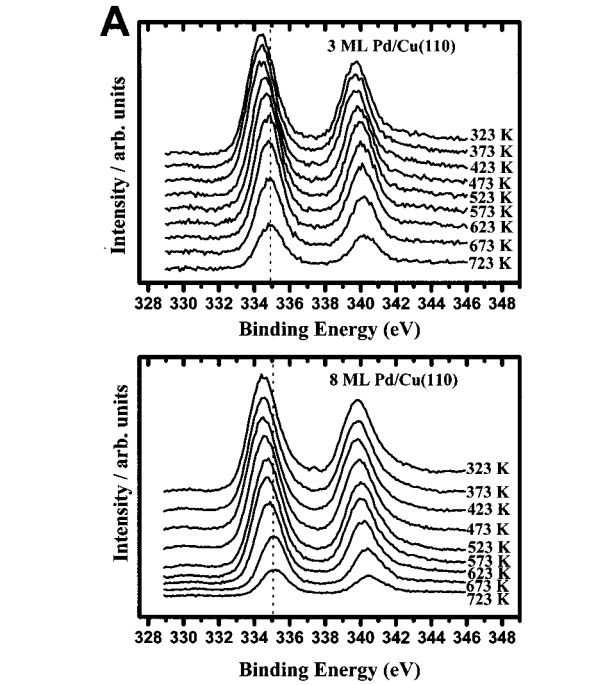

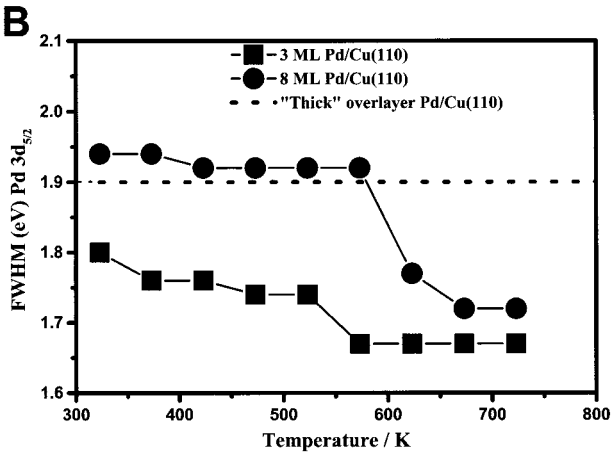

Figure 6. (a) Palladium 3d XPS core levels for 3 and 8 ML films as a function of annealing temperature. (b) Variation of the fwhm as a function of annealing temperature for the 3 and 8 ML films.

Figures 8 to 11 represent the effect of annealing on the morphology of the Pd films. The general procedure followed in these measurements was to anneal the films to temperatures of 500, 600, and 720 K for 30 s with images recorded at ambient temperature. The heating was performed sequentially on the same Pd film. The first annealing temperature (500 K) represents a temperature at which minimal change has occurred with respect to XPS ratios. In contrast, 600 K represents a temperature at which alloying is activated yet is incomplete. The highest annealing temperature (720 K) is sufficient for bulk intermixing to be driven to completion.

Figure 8 illustrates images from the 1 ML films. Little change occurs at 500 K on a large scale (as indicated in Figure 8a); that is, the surface still consists of islands and pits with three or more layers separated by atomic height steps. However, atomic resolution imaging of the previously observed (2×1) superstructure was not possible, suggesting that although no gross changes occur it may be possible even at 500 K that Cu capping of the CuPd domains occurs. In contrast, at 600 K, significant changes have occurred in the surface morphology as illustrated in the 100×100 nm image shown in Figure 8b.

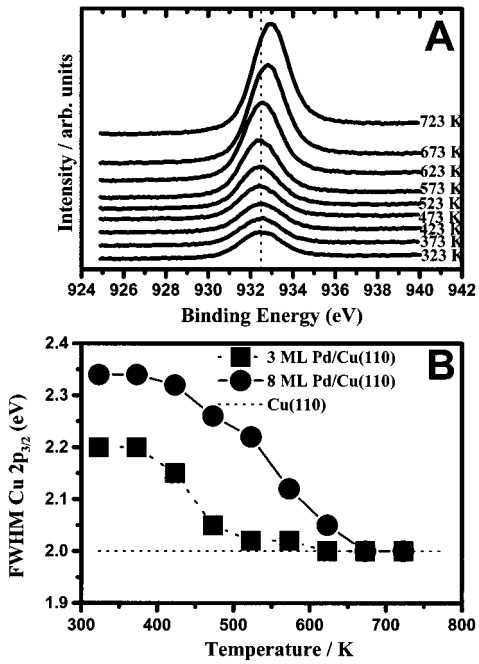

Figure 7. (a) Copper $2p_{3/2}$ core levels for an 8 ML Pd film as a function of annealing temperature. (b) Variation of the Cu $2p_{3/2}$ fwhm as a function of annealing temperature for 3 and 8 ML Pd films.

Terraces appear to elongate with steps between neighboring domains oriented predominantly in the [1$\bar{1}$0] direction. Annealing to 720 K (Figure 8c) leads to a significant flattening of the surface with atomically flat terraces extending for large distances in the [1$\bar{1}$0] direction with shorter terraces in the [001] direction. Figure 9a illustrates the effect of alloying a 2.5 ML Pd film to 510 K. The granular structure of the film is maintained. Figures 9b and c show the effect of annealing to 720 K, where the granular structure is lost and has been replaced by a surface consisting of flat islands separated from neighboring islands by mono-atomic nonlinear steps.

Figure 10a, a 100×100 nm image, illustrates the effect of annealing a 4 ML Pd sample to 500 K. The annealing appears to lead to formation of large islands. Within the islands and in other areas of the surface is a granular structure composed of a number of apparently nucleated (but not Ostwald ripened) Pd clusters. In contrast to the as-deposited film, the clusters adopt a more hemispherical shape with an average diameter of $\sim$30 Å. Further annealing to 600 K (Figure 10b) leads to loss of the Pd clusters and formation of a surface consisting of atomically flat islands of irregular shape with neighboring terraces separated by mono-atomic steps. Small monolayer deep "pits" of varying shape and size also appear within the terraces. Figure 10c illustrates a higher resolution image of the 600 K annealed surface showing the formation of "strings" or atomic chains along the [1$\bar{1}$0] direction. Figure 10d reveals this atomic phenomenon more clearly. Finally, annealing to 720 K results in a further flattening of the surface, as shown in Figure 10e. Again, a multilayer surface is formed with a meandering step direction. Interestingly, a longer-range superstructure becomes apparent in the form of dark lines that run parallel to the [001] direction with an average spacing of between 100 and 200 Å. Such structures have been previously observed for the Cu/Pd(110) system,[11] with their origin proposed to be due to the 7.7% lattice mismatch between the Pd(110) surface and the growing Cu film. The XPS presented here indicates significant alloying for films annealed at high temperature, with the surface consisting of a mixed dilute CuPd alloy phase that desorption

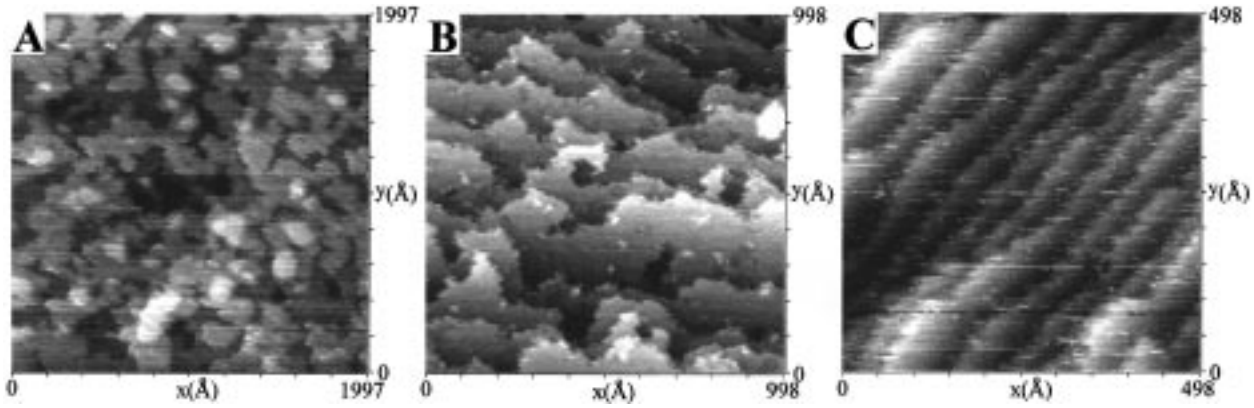

Figure 8. STM images characterizing the structural change of a 1 ML Pd film grown at room temperature on Cu(110) upon annealing to (a) 500 K, (b) 600 K, and (c) 720 K, with subsequent cooling to room temperature before imaging. Tunneling current = 1 nA (all images); bias voltage = 500 mV (a) and 1000 mV (b,c).

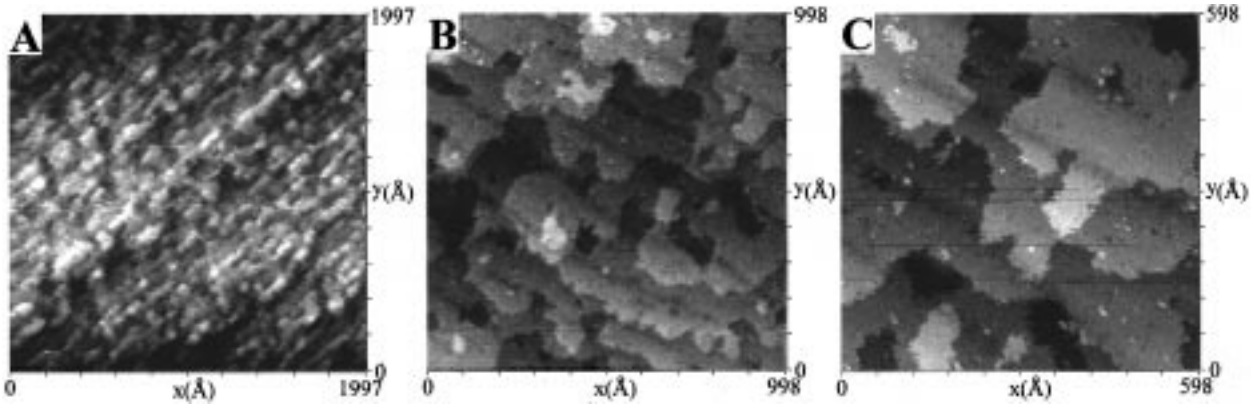

Figure 9. Selected STM images illustrating the effect of annealing on the film morphology for a 2.5 ML film heated to increasingly high temperature and subsequently re-cooled before imaging. (a) 500 K; (b) and (c) after heating to 720 K. Tunneling current = 1 nA (all images), bias voltage = 500 mV (a) and 1000 mV (b,c).

measurements indicate is capped by a Cu monolayer. It is therefore perhaps more likely that the long-range structure is due to mismatch between either the CuPd alloy and the underlying Cu(110) bulk or between the Cu capping monolayer and an underlying CuPd alloy[10] in this particular case. Finally, Figure 11 shows a 10 ML Pd film annealed to 500 K, and again illustrates that no major morphological changes occur for the lowest temperature anneal. Heating to 610 K leads to a surface consisting of small flat terraces (Figure 11b) with a staircase-type structure. The high-temperature anneal leads to formation of flat domains of irregular shape separated from neighboring atomically flat domains by single atomic height steps with highly nonlinear step edges.

3.3 Reactivity of Pd/Cu(110) Overlayers. The surface reactivity of the Cu/Pd surfaces was investigated through adsorption of formic acid on various Pd/Cu(110) surfaces with subsequent decomposition being monitored by TPD. Formic acid (HCOOH) decomposition has been widely employed as a means of probing model catalysts[31,32] and is well documented on Cu(110)[31−35] and Pd(110).[36] On Cu(110), adsorption at low temperature occurs molecularly. As the temperature is raised, the bond to the acidic hydrogen breaks, producing an adsorbed formate intermediate and chemisorbed atomic hydrogen. The formate is stable up to ∼440 K when simultaneous desorption of H_2 and CO_2 occurs in a decomposition limited TPD peak. Hence, the temperature of CO_2/H_2 desorption may be used to monitor the stability of the formate intermediate. The adsorbed formate species is orientated parallel to the close-packed [1$\bar{1}$0] direction with the two oxygens bound to the surface in locally identical sites.[35] This simple reaction mechanism for formic acid adsorption/desorption on Cu(110) is summarized as follows:

$$HCOOH_{(g)} \rightarrow HCOOH_{(ads)}$$

$$HCOOH_{(ads)} \rightarrow HCOO_{(ads)} + H_{(ads)}$$

$$2H_{(ads)} \rightarrow H_{2(g)}$$

$$2HCOO_{(ads)} \rightarrow 2CO_{2(g)} + H_{2(g)}$$

In contrast, formic acid adsorbed on Pd(110) produces simultaneous CO_2/H_2 desorption at 237 K, indicating that formate is much less stable on Pd(110).[36] We refer to "stability" of formate as a measure of the formate reactivity to dehydrogenation (which is the only decomposition pathway seen here).

Figure 12 illustrates the TPD spectrum of formic acid monitoring CO_2 evolution (mass 44) for a range of Pd coverages. Pd/Cu(110) surfaces were preannealed (500 K) prior to room temperature formic acid dosing to minimize compositional/morphological changes during the TPD ramp. In the case of the 1 ML Pd films, coincident CO_2 and H_2 desorption evident at ∼430 K is clearly indicative of formate decomposition. This desorption is quite similar to that observed for Cu(110) other than a slight shifting of the desorption peak maxima to lower temperature, which indicates a de-stabilization of the formate intermediate. Similar TPD were recorded for surfaces annealed to higher temperatures (up to 600 K).

From Figure 12 it is clear that a slight decrease in formate stability is apparent for the low coverage Pd/Cu(110) systems (1 and 2.5 ML Pd). The temperature of CO_2 desorption decreases

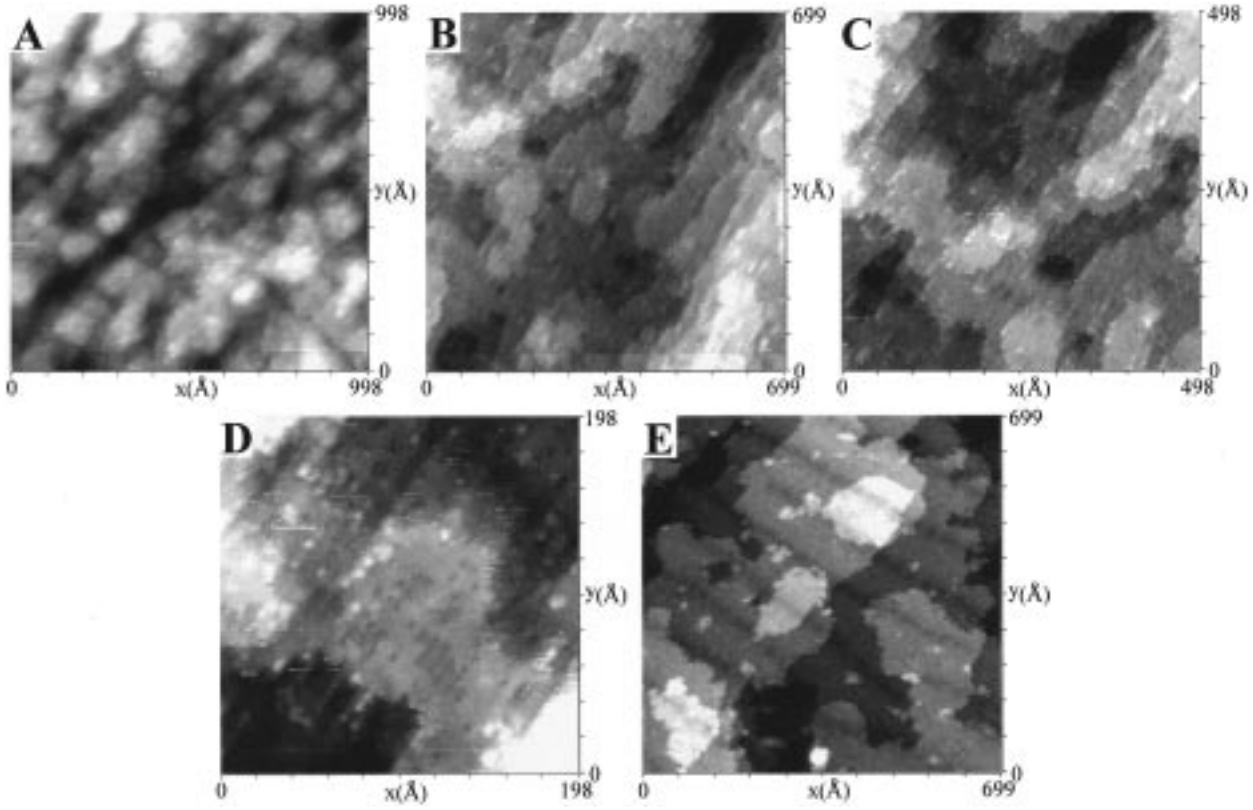

Figure 10. Representative STM images depicting the effect of annealing on the morphology of a 4 ML film heated to increasingly high temperature (sample re-cooled before imaging): (a) the surface morphology at 500 K; (b), (c), and (d) that at 600 K; and (e) that at 720 K. Tunneling current = 1 nA (all images); bias voltage = 500 mV (a−d) and 1000 mV (e).

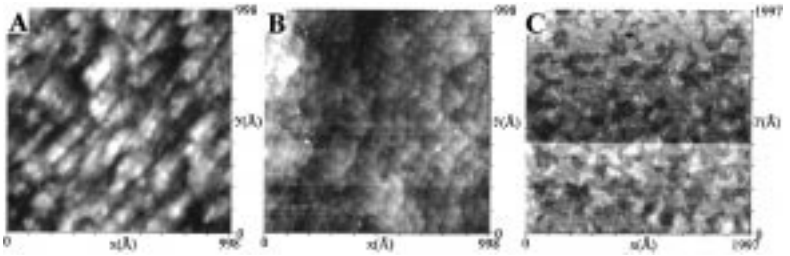

Figure 11. Selected STM images illustrating the effect of annealing on the film morphology for a ∼10 ML film heated to increasingly high temperature. (a) 500 K; (b) 600 K; and (c) 720 K. Tunneling current = 1 nA (all images); bias voltage = 1000 mV (all images).

from 445 K for pure Cu(110) to ∼430 K for a 2.5 ML Pd/Cu(110) annealed alloy surface. In activation energy (E_d) terms, this decrease corresponds to a reduction of only ∼3 kJ mol^{-1} in the thermal stability of the formate compared with Cu(110). Table 1 documents the activation energy for formate decomposition from various surfaces.

Higher coverages of Pd (i.e., 4 and 8 ML) result in TPD profiles that reveal considerable loss in formate stability. In these cases, CO_2 evolution occurred at ∼360 K with no evidence of Cu(110)-like states, corresponding to a ∼22 kJ mol^{-1} reduction in activation energy. Desorption from such high coverage Pd surfaces without prior annealing revealed only Pd-like characteristics with only CO desorbed above room temperature, suggesting that annealing to 500 K already leads to the transformation from a Pd-like outer layer to a layer with considerable Cu character. This intermediate activity (intermediate between elemental Cu and Pd) would seem to be the product of a bimetallic surface layer.

As already mentioned, the low coverage Pd/Cu(110) system (1, 2.5 ML Pd) exhibits a dominant CO_2 desorption peak quite similar in temperature to Cu(110), although there is a significant tailing on the low-temperature side of the peak. In the case of a CuPd[85:15](110) bulk alloy with an ordered CuPd second alloy layer below a Cu terminated surface, which is geometrically similar to Cu(110), it was observed that formate decomposition was very similar to that of pure Cu(110).[37] Thus, we conclude that although preannealing to 500 K has relatively little effect in XPS spectra terms, it leads to capping of the surface by Cu. This conclusion is in keeping with STM results for 500 K annealed films that show no evidence of a (2 × 1) CuPd alloy surface layer.

On the other hand, intermediate formate stability is clearly evidenced for the high coverage Pd/Cu(110) alloy systems (4, 8 ML Pd). The intermediate CO_2 desorption peak is neither Cu- nor Pd-like, suggesting that an alloy state dominates its surface chemistry. Referring to Table 1, it is clear that this alloy state exhibits similar desorption characteristics to the PdCu(110) alloy with a Cu/Pd surface region of 0.55 ± 0.05 as observed by Holroyd.[38] Several models have been proposed to explain this intermediate activity although they tenuously suggest that for such a large shift in formate stability the most probable scenario is a so-called 'interatom' bidentate formate intermediate bound to both a Cu and a Pd atom simultaneously.[38] Whether this adsorbed species is possible is unknown, although the bridging

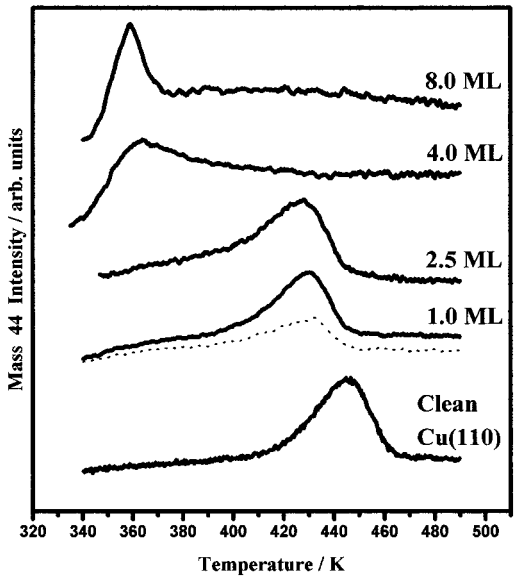

Figure 12. Mass 44 (CO_2) TPD spectra from clean Cu(110) and for Pd films of (a) 1 ML [coincident H_2 (mass 2) desorption (dotted line)]; (b) 2.5 mL; (c) 4 ML; and (d) 8 mL. All Pd films were preannealed to 500 K and re-cooled to 300 K prior to dosing with saturation formic acid coverage (~10 Langmuirs).

TABLE 1: Comparison of the Activation Energy (E_d) for Formate Decomposition on Various CuPd Model Catalysts[a]

substrate	β, K s^{-1}[b]	T_{max}, K	E_d, kJ mol^{-1}
Pd(110)	3.0	237	60
Cu(110)	1.8	445	117.7
1−2.5 ML Pd/Cu(110)	1.2	430	115
4 ML Pd/Cu(110)	1.5	363	95.9
8 ML Pd/Cu(110)	1.2	358	95.2
CuPd[85:15](110)	2.65	445[d]	116.2
CuPd[50:50](110)	2.5	346[e]	89.8

[a] Calculated using the Redhead approximation, with a pre-exponential factor $\nu = 10^{-13}$ s^{-1}, assuming the reaction follows first-order kinetics. [b] Heating rate. [c] Reference 36. [d] Reference 43. [e] Reference 38.

bidentate formate bonding structure is known to be the most favored on Cu(110).[39]

The effect of further annealing (600 K) on the higher coverage Pd samples (4, 8 ML Pd) was also examined. Figure 13a reveals the variation in chemical reactivity of a 4 ML Pd/Cu(110) surface upon annealing from 500 to 600 K. The spectrum obtained after annealing to 600 K illustrates some interesting points, the most striking being the presence of two distinct CO_2 desorption states. The first peak corresponding to the alloy state (~360 K) and a second peak found at ~420 K. This latter state is to some extent Cu-like in origin. For the 4 ML Pd film, the presence of mixed desorption peaks upon annealing to 600 K suggests that one of the surface components is Cu-like (i.e., Cu surface islands exist leading to the high-temperature desorption peak at ~420 K perturbed by Pd in deeper layers). The fact that the CuPd alloy state persists (~360 K) suggests mixed CuPd regions are still present in the outermost layer.

Finally, the CO_2 desorption from a 8 ML Pd film preannealed to 500 K exhibits a well-defined narrow peak (Figure 13b) at ~360 K. This peak shape suggests that only one adsorption/desorption site is present for the formate. Unlike the less Pd-rich surfaces, this rules out a random dilute CuPd alloy system and would support a surface region consisting of a more homogeneous alloy top layer. Upon annealing to 600 K, a broadening of the alloy-state peak occurs, suggesting a number of locally different CuPd alloy sites in the surface layer (as shown in Figure 13b). Annealing of this surface layer (including any lower Pd coverage surface) to even higher temperature (~720 K) does, however, lead to a surface with desorption properties similar to clean Cu(110).

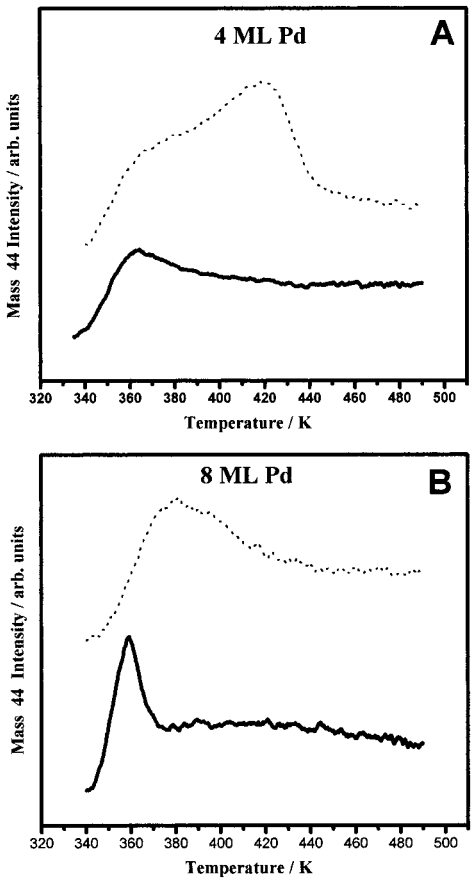

Figure 13. Effect of annealing a Pd film of (a) a 4 ML and (b) an 8 ML film to 500 K (full line) and 600 K (dotted line) on formate thermal stability.

4. Discussion

The general growth mechanism of Pd on Cu(110) at 300 K is suggestive of growth of high-density, flat-topped Pd clusters above a bi- or trilayer mixed CuPd interface. The initial observation of growth of considerable areas of a p(2 × 1) CuPd top layer at coverages ~1 ML can be understood on the basis of the model suggested by Murray et al. for low Pd coverages that consisted of an outermost Cu layer covering a p(2 × 1) CuPd underlayer with the occurrence of "capping" of the growing Pd film to minimize the surface energy. Thus, incoming Pd atoms at coverages ≥0.5 ML will impinge largely on a Cu outermost layer. The most likely scenario is that Pd substitutes within the outermost Cu monolayer, pushing Cu islands above so the Cu can then alloy with more Pd, forming an intermixed bi/trilayer. At this stage, arriving Pd is inhibited from further mixing with the Cu because of the mixed CuPd buffer layer. Hence, pure Pd islands begin to grow above the mixed interface. Such a growth mechanism is quite different than that proposed for Cu on Pd(110)[11−14] where little intermixing appears to occur, rather the first monolayer is suggested to grow pseudomorphically and epitaxially, capping the Pd substrate, as expected from the higher surface energy of Pd compared with that of Cu.

An interesting point in comparison with the STM work of Hahn et al.[11] for Cu on Pd is their observations of a large period structure revealed as repeating dark lines across the STM image

that the authors assign to strain mismatch of the pure Cu film to the Pd(110) substrate (7.7% lattice mismatch). We observe similar long period structures for the Pd/Cu(110) system after annealing to 725 K when CuPd intermixing is complete, as determined by XPS, so we cannot invoke a similar film/substrate mismatch argument. In our case, it is likely that the long period structure in our images is due to a mismatch of the "capping" Cu monolayer with the underlying CuPd alloy which stems from the differing lattice parameters of a Cu monolayer and a CuPd alloy. However, as already mentioned, the possibility of mismatch between CuPd alloy and underlying Cu substrate cannot be ruled out. Thus, it would be expected that the period would be larger than for Cu on Pd(110) because of the smaller mismatch between an alloy and pure metal. This expectation is indeed what is observed, with the period being >100 Å compared with that of ~80 Å observed by Hahn et al.

The XPS core level data in the form of peak binding energy position as a function of coverage and annealing temperature allows further insight into the nature of the CuPd interface. Previous studies on CuPd alloys indicate that large shifts to higher binding energy occur in the Pd $3d_{5/2}$ core level relative to pure Pd. Shifts of ~0.75 eV have been measured for a Pd_8Cu_{92} alloy and a ~0.45 eV shift was recorded for a $Pd_{40}Cu_{60}$ bulk alloy,[40] with a recent cluster calculation reproducing the concentration-dependent shift for the aforementioned alloys. Therefore, on this basis, we would expect the Pd 3d binding energy to be highly sensitive to changes in the Pd environment, undergoing a considerable shift to higher binding energy when a metallic-like Pd film is transformed into a dilute alloy via annealing.

For films deposited at 300 K, it is likely that the relatively large escape depth of the Pd $3d_{5/2}$ electrons (16.7 Å [24]) will lead to the 3d envelope containing contributions from Pd atoms in a range of environments including pure Pd clusters (bulk and surface atoms) and alloyed interface Pd. At low Pd coverages (≤1 ML), if our postulated model of an intermixed CuPd alloy is correct, we would expect to find a high binding energy peak of narrow fwhm (due to Pd in a single alloyed environment). Increasing weight should occur on the low binding energy side of the peak as metallic Pd clusters grow above the mixed interface, with a shift in the peak maximum to lower binding energy at high coverages where the metallic Pd begins to dominate. Indeed, in Figure 3 we see growth of a high binding energy peak (~334.8 eV) for coverages up to ~1 ML when CuPd alloying readily occurs, with subsequent additional emission at lower binding energy because of metallic Pd clusters at ~334.4 eV. Hence, the XPS data fully supports our mechanism for growth of a mixed CuPd alloy interface up to ~1 ML coverage followed by growth of pure Pd clusters.

In contrast, annealing the Pd film, which promotes intermixing at temperatures above ~500 K as shown by the decreasing Pd/Cu XPS ratio, would be expected to reveal a decrease in the Pd 3d fwhm due to the loss of Pd clusters. Such a decrease is clearly observed between 500 and 600 K. Annealing to high temperatures yields a dilute CuPd alloy that should in turn show a shift in the core-level binding from lower (pure metallic Pd clusters dominating for high coverage 300 K films) to higher values as a dilute CuPd alloy is formed. Again this prediction is indeed what takes place, with a clear reduction in the fwhm between 500 and 600 K and with a loss of peak weight at the low binding energy signifying the dissolving of the Pd clusters into the Cu substrate. Net upward shifts of 0.5 ± 0.1 and 0.7 ± 0.1 eV are observed for the Pd 3d core-level of 725 K annealed films of 3 and 8 ML Pd, respectively, when compared with the room-temperature deposit. This result is consistent with formation of a dilute CuPd alloy.

A smaller shift to higher binding energy (0.3 ± 0.1 eV) is observed for the Cu $2p_{3/2}$ core-level upon intermixing along with a clear decrease in the fwhm, which is already beginning at ~400 K. Interestingly, a plot of the variation in intensity of the Cu $2p_{3/2}$ core-level for Pd films of 3 and 8 ML coverage indicate a significant increase in the Cu $2p_{3/2}$ intensity between 400 and 500 K, whereas the Pd $3d_{5/2}$ intensity remains unaltered. This difference is perhaps indicative of out-diffusion of Cu to alloy with, or to encapsulate, areas of overlying Pd clusters, a point of considerable importance when addressing the desorption behavior of the formate intermediate.

As previously mentioned, formate decomposition on Cu(110) was observed and identified by the simultaneous desorption of CO_2 and H_2 in a decomposition limited peak at 445 K ($\beta = 1.8$ K s^{-1}). The temperature of the desorption peak may be utilized to estimate the formate stability, and the decomposition activation energy has been found to be 118 kJ mol^{-1} using the Redhead approximation.[41] In comparison, Pd(110) is much more active toward formate dehydrogenation. Aas et al.[36] report simultaneous desorption of CO_2 and H_2 for formic acid adsorbed at low temperature in a decomposition-limited peak at 237 K ($\beta = 3$ K s^{-1}) with the desorption following first-order kinetics and exhibiting an activation energy of 60 kJ mol^{-1}. Molecular CO remains on the surface above 250 K, yielding a desorption limited peak at ~470 K.

At low Pd coverages (1 and 2 ML), following a preanneal to 500 K, co-incident CO_2/H_2 desorption at ~430 K is observed that is indicative of a decomposition-limited fragmentation of a formate intermediate rather close to that for a pure Cu(110) surface although a small destabilization of the formate is apparent.

Newton and co-workers[37] have studied the thermal decomposition of formic acid on a $Cu_{0.85}Pd_{0.15}(110)$ bulk alloy. The structure of the surface that exhibits a (2×1) superstructure in LEED has been the focus of considerable attention.[21,37,42−45] It has been unequivocally demonstrated that the (2×1) periodicity has its origin in chemical ordering between Cu and Pd in the second layer in the form of a mixed 50:50 s layer with Pd atoms occupying every second site along the close packed $[1\bar{1}0]$ rows. The top layer is Cu-rich.[42,43] Newton et al. observed a co-incident CO_2/H_2 TPD peak at 445 K ($\beta = 2.65$ K s^{-1}) along with a small amount of molecular formic acid desorption. Again, using the Redhead approximation and assuming first-order kinetics, an activation energy of 116 kJ mol^{-1} is calculated and found to be slightly less than that determined for Cu(110) (118 kJ mol^{-1}). Therefore, the inclusion of Pd in the second layer of the alloy leads to an increase in the reactivity toward dehydrogenation of the formate relative to Cu(110).

A possible explanation of the similarity of the formate decomposition from the low Pd loading films with that of the $Cu_{0.85}Pd_{0.15}(110)-(2 \times 1)$ alloy is that the preannealing to 500 K leads to a pure or almost pure Cu layer capping a mixed CuPd alloy. A recent STM study of Pd deposition ($\theta_{Pd} = 0.5$ mL) on Cu(111) at ~530 K led to a surface with Pd atoms substituted into the top Cu layer with roughly half of the Pd atoms subsurface.[46] As it is likely that place exchange on the close-packed (111) surface will have a higher activation energy than on the more open (110) surface, capping of the Pd films upon annealing to 500 K for a short period is quite possible.

At higher Pd coverages (4 and 8 ML), a considerable destabilization of the formate intermediate occurs, which is indicative of a surface intermediate in stability between pure

Cu and Pd(110). Auger data for the thicker Pd films suggests that significant changes in surface composition do not occur upon annealing to 500 K. This observation is backed up by STM data, which attests that the Pd morphology is not significantly altered upon annealing to 500 K for a short period. It is thus surprising that the formate stability remains intermediate between Cu and Pd if the surface were to consist of pure Pd clusters in the 4 and 8 ML films. The fact that the formate decomposition kinetics do not resemble those of Pd(110) suggests that although the surface is still dominated by Pd clusters, Cu atoms are present within the outermost layer. The presence of Cu atoms leads to large changes in the Pd valence band structure in the form of withdrawal of the d-partial density of states on Pd sites from the Fermi level. The exact d-density of states at the Fermi level is critically dependent on the CuPd stoichiometry, and recent work indicates that withdrawal is effectively complete at a CuPd stoichiometry of 1:1.[47] Hence, we propose that annealing the thicker films to 500 K leads to out-diffusion of Cu from the mixed CuPd interface to partially cover the Pd clusters, resulting in an outermost mixed CuPd surface with intermediate formate desorption kinetics. Previous work on a Cu(100)-c(2 × 2) Pd surface alloy, for which significant Pd is present in the outermost layer, gave evidence of a large destabilization in the CO desorption activation energy to 300 K, a value intermediate between pure Pd(100) and Cu(100) in which the main CO desorption peak occurs at 500 and 170 K, respectively.[26,48] This result further attests to the fact that a mixed CuPd outermost layer leads to an adsorbate stability intermediate between the two pure metals.

5. Conclusions

A complex growth mechanism for Pd on Cu(110) has been demonstrated in which initial growth occurs via intermixing to form an ordered CuPd(2 × 1) surface alloy of two to three layers thickness and a heterogeneous surface consisting of monolayer high 2D islands and monolayer deep "pits". Subsequent growth takes place in the form of densely packed Pd platelets. The platelets have a large base-to-height ratio and vary in shape and size, although some preference for rectangular islands aligned with their edges parallel to the high-symmetry substrate directions is detected.

XPS data has shown that rapid alloying occurs at temperatures between 500 and 600 K due to interdiffusion of Pd into the Cu substrate. Although not readily detected by XPS, capping of the resulting CuPd alloy by a low-surface-energy Cu monolayer is suspected, as indicated by STM and formate decompostion measurements, for temperatures as low as 500 K. Temperature-induced morphological transformations have been followed by STM, which indicates that the granular platelet structure of the higher-coverage Pd films is maintained upon heating to 500 K without significant Ostwald ripening or cluster coalescence. However, the following large changes are induced by heating to 600 K and beyond: the granular Pd film is lost, transforming into a multilevel surface with large flat domains bounded by nonlinear mono-atomic steps with areas of raised islands and large pits formed by Pd substitutionally transplanting into the Cu lattice; and the ejected Cu atoms grow as islands and lead to the multilayered structure observed.

Morphological changes are mirrored in XPS core level binding energies and peak widths with a large shift of the Pd $3d_{5/2}$ core level to higher binding energy and an accompanying narrowing of the line width as the transition from a granular metal film to a CuPd alloy is induced. The narrowing in peak width is in keeping with the evolution from a highly heterogeneous Pd environment (surface Pd atoms at cluster edges, bulk Pd atoms within clusters, Pd in an intermixed interface, etc.) to a dilute CuPd alloy where palladium atoms are all in similar local environments. The effect of intermixing (shift to higher binding energy of core levels and narrowing of peak width) leads to XPS spectra similar to those obtained from a 1 ML film consisting of a thin intermixed CuPd interface.

Finally, the reactivity of the CuPd interface has been probed by monitoring the changes in stability of the formate intermediate. Low Pd coverages (1 and 2.5 ML) show only a small destabilizing influence on the formate, suggesting that the surface is largely Cu monolayer capped. Thicker Pd films show a marked destabilization of the formate (decomposition activation energies of 118 and 95 kJ mol^{-1} on Cu(110) and 8 ML Pd film, respectively). This destabilization is attributed to desorption from a mixed CuPd surface, indicating that the stability of the formate intermediate may be altered to a state intermediate between pure Cu and Pd via surface alloy formation.

Acknowledgment. We gratefully acknowledge the support of the EPSRC and the University of Reading. J. P. Reilly acknowledges Dublin City University for provision of travel funds, and P. Stone acknowledges the provision of a case award by Oxford Instruments.

References and Notes

(1) Campbell, C. T. *Annu. Rev. Phys. Chem.* **1990**, *41*, 775 (and references therein).
(2) Bardi, U. *Rep. Prog. Phys.* **1994**, *57*, 939.
(3) Choi, K. I.; Vannice, M. A. *J. Catal.* **1991**, *131*, 36.
(4) Skoda, F.; Astier, M. P.; Pajonk, G. M.; Primet, M. *Catal. Lett.* **1994**, *29*, 159.
(5) Anderson, J. A.; Fernández-Garcia, M.; Haller, G. L. *J. Catal.* **1996**, *164*, 477.
(6) Taylor, R. *J. Inst. Metals* **1934**, *54*, 255.
(7) Jones, F. W.; Sykes, C. *J. Inst. Metals* **1939**, *65*, 419.
(8) Sundaram, V. S.; de Moraes, M. B.; Rogers, J. D.; Kleiman, G. G. *J. Phys. F* **1981**, *11*, 1151.
(9) Winter, H.; Durham, P. J.; Temmerman, W. M.; Stocks, G. M. *Phys. Rev. B* **1986,** *33*, 2370.
(10) Bennett, R. A.; Poulston, S.; Price, N. J.; Reilly, J. P.; Stone, P.; Barnes, C. J.; Bowker, M. *Surf. Sci.*, in press.
(11) Hahn, E.; Kampshoff, E.; Fricke, A.; Bucher, J.-P.; Kern, K. *Surf. Sci.* **1994**, *319*, 277 (and references therein).
(12) Barnes, C.; Gleeson, M. *Surf. Sci.* **1994**, *319*, 157.
(13) Vook, R. W.; Bucci, J. V. *Thin Solid Films* **1988**, *163*, 447.
(14) Li, H.; Tian, D.; Jona, F.; Marcus, P. M. *Solid State Comm.* **1991**, *77*(9), 651 (and references therein).
(15) Murray, P. W.; Stensgaard, I.; Lægsgaard, E.; Besenbacher, F. *Surf. Sci.* **1996**, *365*, 591 (and references therein).
(16) Wu, S. C.; Lu, S. H.; Wang, Z. Q.; Lok, C. K. C.; Quinn, J.; Li, Y. S.; Tian, D.; Jona, F.; Marcus, P. M. *Phys. Rev. B* **1988**, *38*, 5363.
(17) Murray, P. W.; Stensgaard, I.; Lægsgaard, E.; Besenbacher, F. *Phys. Rev. B* **1995**, *52*, R14404.
(18) Fujinaga, Y. *Surf. Sci.* **1979**, *84*, 1.
(19) Fujinaga, Y. *Surf. Sci.* **1979**, *86*, 581.
(20) Murray, P. W.; Thorshaug, S.; Stensgaard, I.; Besenbacher, F.; Lægsgaard, E.; Ruban, A. V.; Jacobsen, K. W.; Kopidakis, G.; Skriver, H. L. *Phys. Rev. B* **1997**, *55*, 1380.
(21) Newton, M. A.; Francis, S. M.; Bowker M. *Surf. Sci.* **1991**, *259*, 56.
(22) Ying, D.; Madix, R. J. *Surf. Sci.* **1979**, *84*, 375.
(23) Moulder, J. F.; Stickle, W. F.; Stickle, P. E.; Bomben, K. D. *Handbook of X-ray Photoelectron Spectroscopy*; Chastain, J., Ed.; Perkin-Elmer: Eden Prairie, MN, 1992.
(24) Briggs, D.; Seah, M. P. *Practical Surface Analysis*; John Wiley & Sons: New York, 1990.
(25) Mezey, L. Z.; Giber, J. *Jpn. J. Appl. Phys.* **1982**, *21*, 1569.
(26) Pope, T. D.; Griffiths, K.; Norton, P. R. *Surf. Sci.* **1994**, *306*, 294.
(27) Graham, G. W.; Schmitz, P. J.; Thiel, P. A. *Phys. Rev. B* **1990**, *41*(6), 3353.
(28) Rao, R. S.; Bansil, A.; Asonen, H.; Pessa, M. *Phys. Rev. B* **1984**, *29*, 1713.
(29) Rodriguez, J. *Surf. Sci. Rep.* **1996**, *24*, 223.

(30) Fernàndez-Garcia, M.; Conesa, J. C.; Coltet, A.; Ricart, J. M.; Lopez, N.; Illas, F. *J. Phys. Chem. B* **1998**, *102*, 141.
(31) Bowker, M.; Madix, R. J. *Surf. Sci*. **1981**, *102*, 542.
(32) Madix, R. J. *Surf. Sci*. **1979**, *89*, 540.
(33) Bowker, M.; Rowbotham, E.; Leibsle, F. M.; Haq, S. *Surf. Sci*. **1996**, *349*, 97.
(34) Poulston, S.; Jones, A. H.; Bennett, R. A.; Bowker M. *Surf. Sci*. **1997**, *377*, 66.
(35) Poulston, S.; Bennett, R. A.; Jones, A. H.; Bowker, M. *Phys. Rev. B* **1997**, *55*, 12888 (and references therein).
(36) Aas, N.; Li, Y.; Bowker, M. *J. Phys.: Condens. Matter* **1991**, *3*, 1.
(37) Newton, M. A.; Bowker, M. *Surf. Sci*. **1994**, *307*−*309*, 445.
(38) Holroyd, R. Ph.D. Thesis, Reading Catalysis Centre, University of Reading, Reading, United Kingdom, 1998.
(39) Puschmann , A.; Haase, J.; Crapper, M. D.; Riley, C. E.; Woodruff, D. P. *Phys. Rev. Lett.* **1985**, *54*(*20*), 2250.
(40) Martensson, N.; Nyholm, R.; Calén, H.; Hedman, J.; Johansson, B. *Phys. Rev. B* **1981**, *24*, 1725.
(41) Redhead , P. A. *Vacuum* **1962**, *12*, 203.
(42) Holmes, D J.; King, D. A.; Barnes, C. J. *Surf. Sci.* **1990**, *227*, 179.
(43) Newton, M. A.; Francis, S. M.; Li, X.; Law, D.; Bowker, M. *Surf. Sci.* **1991**, *259*, 45.
(44) Cottrell, C.; Bowker, M.; Hodgson, A.; Worthy, G. *Surf. Sci*. **1995**, *325*, 57.
(45) Newton, M. A.; Francis, S. M.; Bowker, M. *Surf. Sci*. **1992**, *269/270*, 41.
(46) Pötsche, G. O.; Behm, R. J. *Phys. Rev. Letts.* **1991**, *44*, 1442.
(47) Barnes, C. J.; Gleeson, M.; Sakhrakorpi, S.; Lindroos, M. *Surface Sci.*, submitted.
(48) Valden, M.; Aaltonen, J.; Pessa, M.; Gleeson, M.; Barnes, C. J. *Chem. Phys. Lett.* **1994**, *228*, 519.